

Analysis of Mixing Chambers for the Processing of Two-Component Adhesives for Transport Applications

P. Steinert^{*1}, I. Schaarschmidt¹, R. Paul¹, M. Zinecker¹, M. Hackert-Oschätzchen¹, Th. Muschalek², J. Esslinger², A. Schubert¹

¹Professorship Micromanufacturing Technology, Chemnitz University of Technology, 09107 Chemnitz, Germany

²Rublic+Canzler GmbH, 01067 Dresden, Germany

*Corresponding author: philipp.steinert@mb.tu-chemnitz.de

Abstract:

At the Chemnitz University of Technology innovative system technology for the user-friendly, mobile and energy-efficient processing of two-component adhesives using electrically driven ejection is developed. In this context, the simulation-based layout of main components for the achievement of high mixing intensity as well as the reduction of power demands are key challenges.

In the present study a fluid-dynamic simulation model of a pre-mixing chamber with two inlets for a main adhesive component and an accelerator component was established. Mass transport equations for the diffusive and convective mixing of the adhesive components were implemented and evaluated with regard to calculation effort and information content. Further assessments of the phase distribution were realized under consideration of varying operation conditions. With the simulation results a suitable inlet design for the accelerator component injection could be identified.

Keywords:

Fluid Mixing, Two-component Adhesives, Pressure Loss

1. Introduction

Two-component adhesives are commonly used for joining and sealing in transport applications particularly in the wide field of body construction. Adhesive bonds exhibit high mechanical strength because of the resulting homogeneous stress distribution. Furthermore, modern adhesives can withstand thermal and chemical influences and can be processed rapidly in series production [1].

Multi-component adhesives are frequently processed by handgun systems at fixed workspaces. For the industrial purpose, pressurized air is usually used as energy source for squeezing and mixing of the

adhesive components [2]. However, these systems feature high maintenance costs and rather limited usability for the mobile operation, e. g. for repair or construction work outside a manufacturing plant.

In cooperation with Rublic+Canzler GmbH (Germany), the Chemnitz University of Technology develops new concepts and technologies for the mobile processing of two-component polyurethane based adhesives. In contrast to conventional pneumatic systems, the development is concentrated on the much more practicable, electric drive technology (Fig. 1).

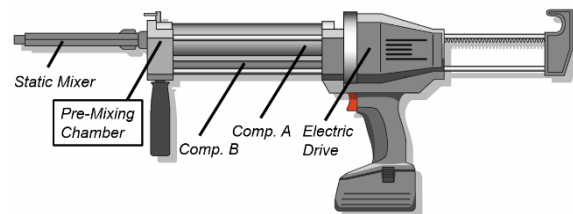


Figure 1. Application for the mobile processing of two-component adhesives.

For an electrically driven mixing application for two-component adhesives, a high mixing intensity and low power demands in the fluid technical components are required. In the present study the pre-mixing chamber (see Fig. 1) of the application was analyzed and geometrically dimensioned by the help of different parameters characterizing the pressure loss and power demand on the one hand and the mixing intensity on the other hand.

2. Numerical Model

2.1 Specification

In the pre-mixing chamber the separate fluid components are combined to one mass flow by injection of the accelerator component B into the mass flow of main component A. The principle and geometry of this mixing chamber is shown in Fig. 2.

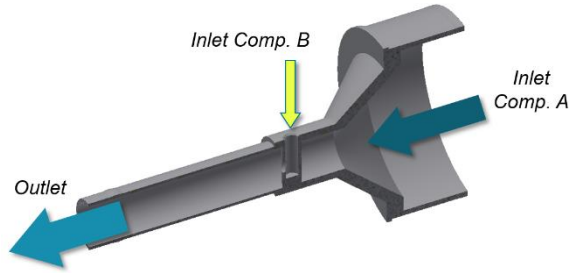





Figure 2. Geometry and function principle of the pre-mixing chamber.

Because of the given assembly space, the outlet diameter of 12 mm, the diameter of the component A inlet of 47 mm and the total length of 93 mm were fixed. However, the component B supply was geometrically free and therefore varied in three steps with the aim to validate the effect on the mixing behavior and the power demand. Note, a diameter enlargement of the component B inlet decreases the flow cross-section along the path component A \rightarrow outlet and increases it along the path component B \rightarrow outlet (see Tab. 1). This is valid for the reduction of the diameter vice versa. The geometry variation is illustrated in Tab. 1.

Table 1: Defined parameter variation

Parameter	Option -small-	Option -medium-	Option -large-
Illustration			
Inner Pipe Diameter $d_{i,B}$	1.7 mm	3.2 mm	4.8 mm
Outer Pipe Diameter $d_{o,B}$	3.2 mm	4.8 mm	7.2 mm
$v_{A,inj}/v_{B,inj}$	0.34	1.28	3.17

The parameter $v_{A,inj}/v_{B,inj}$ characterizes the ratio of the adhesive component velocities in the area of injection. The calculated values indicate that the velocity of the component B is much larger than that of component A in the injection area with the small option. In the cases of medium and large injection pipe, the velocity of component A becomes larger than that of component B because of the smaller flow area.

2.2 Governing Equations

By estimating the Reynolds number at the outlet, it was found that Re amounts to a value quite a few orders of magnitude below the critical value of 2300 for pipe flow. For this reason incompressible, stationary Navier-Stokes equations were applied in this study for the calculation of the laminar flow field:

$$\rho(\vec{v} \nabla) \vec{v} = -\nabla p + \eta \nabla^2 \vec{v} \quad (1)$$

$$\rho \nabla \vec{v} = 0 \quad (2)$$

Beside the flow parameters, the mass transport of the two adhesive components was represented by the stationary convection-diffusion equation:

$$\vec{v}(\Phi \vec{v}) = \vec{v}(\nu \vec{\nabla} \Phi) \quad (3)$$

As becomes clear, the volume fraction Φ was applied as transport parameter. In this context it was defined that Φ describes the ratio of component B into the fluid domain with a value range of $0 \leq \Phi \leq 1$.

The solution of the equations was carried out by a two-stage approach, where the laminar flow field was solved without the convection-diffusion equation at first. After that laminar flow and mass transport were solved together using the segregated solution procedure and the solution of the first step initially.

2.3 Boundary Conditions and Material Properties

With the aim to use the geometry shown in Fig. 1 for fluid dynamics simulations the corresponding fluid domain was determined by commercial CAD software. In this context the model was simplified because of the symmetric design. However, the conical inlet of component A was not simplified or neglected because of the significantly changing shear rate in this area. Together with the strongly pseudoplastic viscosity characteristics of the adhesive components which were measured and implemented in the model, the pressure change along the conical entrance of component A could not be described analytically.

The material properties of the adhesive components were implemented according to technical data sheets and measurements, whereas the unknown diffusion coefficient was selected by estimation.

The volume flows were prescribed with mixing ratios of $M = 100:6$ (A:B) as typical ratio and $M = 100:14$ (A:B) additionally as maximum possible ratio concerning to the manufacturer specifications. With a usual processing speed, a

volume flow of about 7 ml/s and a mean flow velocity of approx. 6 cm/s are achieved in the outlet of the pre-mixing chamber.

Beside the two adhesive components a mixing fluid was introduced. This definition was used for the description of the fluid properties in the range of $0 < \Phi < 1$. Both, density and dynamic viscosity of the mixing fluid were calculated based on the phase fraction.

The walls of the pre-mixing chamber were set to the no slip boundary condition. For the calculation of the phase distribution, the inlets of components A and B were predefined with the concentrations of $\Phi = 0$ and $\Phi = 1$, respectively. Further boundary conditions and the initial phase boundary are shown in Fig. 3.

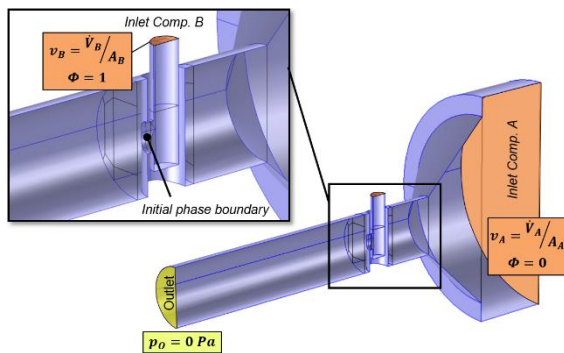


Figure 3. Defined boundary conditions and initial phase boundary.

2.4 Mesh

A high mesh quality was assured by applying structured meshes in a wide range of the fluid-dynamical domain. In the geometrically complicated area of component B injection, meshing with refined tetrahedral elements was performed. The maximum element size did not exceed a maximum value of 0.2 mm. Depending on the geometry the final meshes consisted of approx. 550k elements.

4. Simulation Results

4.1 Phase distribution

The simulation results were analyzed primarily concerning phase distribution of the components on the one hand and power demand on the other hand. To begin with the phase distribution, the transport of component B is illustrated in Figs. 4–6 using streamlines in gray color. Streamlines can be used for visualization because of the low amount of diffusion in the simulations. The images in Figs. 4–6 show furthermore the velocity field of component A in the injection pipe.

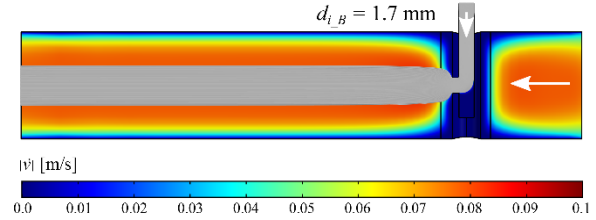


Figure 4. Velocity field and component B streamlines for $d_{i,B} = 1.7$ mm and $M = 100:6$.

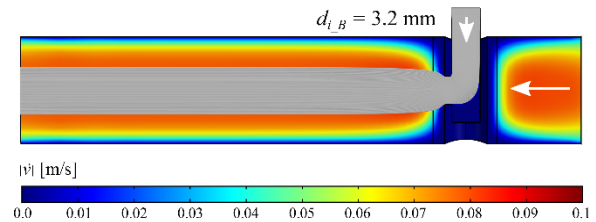


Figure 5. Velocity field and component B streamlines for $d_{i,B} = 3.2$ mm and $M = 100:6$.

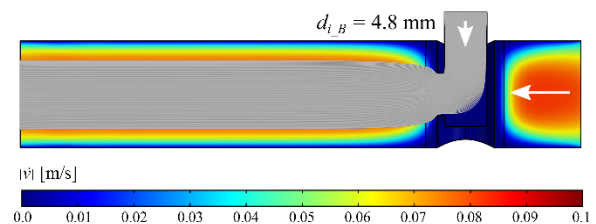


Figure 6. Velocity field and component B streamlines for $d_{i,B} = 4.8$ mm and $M = 100:6$.

In order to validate the role of diffusion on the one hand and the influence of varying operation conditions on the other hand, the phase distributions at the outlets were depicted, see Fig. 7. In these plots blue color indicates the presence of component A ($\Phi \leq 0.5$) while the red contour lines suggest the interface between the two components ($\Phi = 0.5$). In addition to that the streamlines were illustrated in gray color once more. By the help of these figures it becomes clear, that the phase distribution is well approximated by streamlines because of the low diffusion transverse to the flow direction. The low dwell time of the fluids in the pre-mixing chamber as well as their relatively large viscosities confirm the obtained results theoretically.

Regarding Fig. 7a-c the geometrical extent of the component B region in vertical direction clearly increases with increasing diameter $d_{i,B}$. By the help of measurements it was found that the increase in vertical direction amounts to 70 % at $d_{i,B} = 4.8$ mm in comparison to the smallest diameter of $d_{i,B} = 1.7$ mm. For the phase distribution with the

mixing ratio of $M = 100:14$, this tendency still remains. However, the improvement compared to the case $M = 100:6$ is lower with an increase of approx. 25 % from $d_{i_B} = 1.7$ mm to $d_{i_B} = 4.8$ mm.

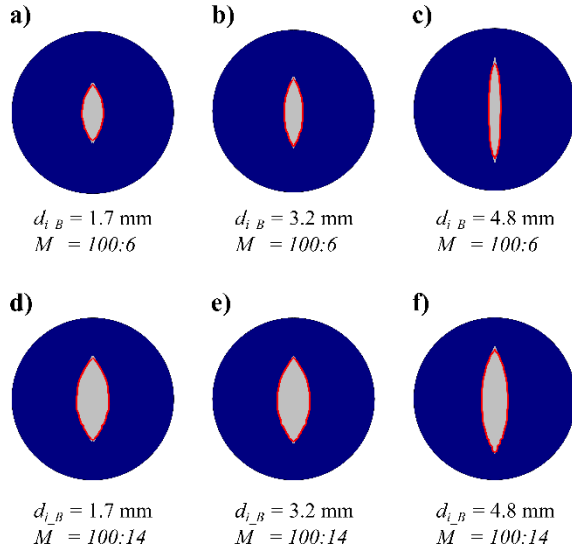


Figure 7. Phase distributions Φ at the outlet for the three tested diameters d_{i_B} and different mixing ratios M .

With a view to the target design of the mixing application (Fig. 1), the third case may be the most favorable. In particular the larger geometrical extent of the mixing region will be advantageous for the mixing efficiency in the main mixing stage using static mixers. By the help of a suitable pre-mixing the dimensioning of the main mixers can be realized with less mixer elements and significantly lower pressure drop.

4.2 Power demand

Power demands due to viscous friction were described by the pressure losses between the two inlets and the outlet. By using these pressure losses, the hydraulic power for the mixing of the adhesive components in the pre-mixing chamber can be determined by the following equation (for $p_0 = 0$ Pa):

$$P_H = \dot{V}_A \bar{p}_A + \dot{V}_B \bar{p}_B \quad (4)$$

For the typical mixing ratio of $M = 100:6$ the evaluation yields the result that is illustrated in Fig. 8. As expected the power demand along the path component A \rightarrow outlet increases and that along the path component B \rightarrow outlet decreases continuously with increasing diameter d_{i_B} .

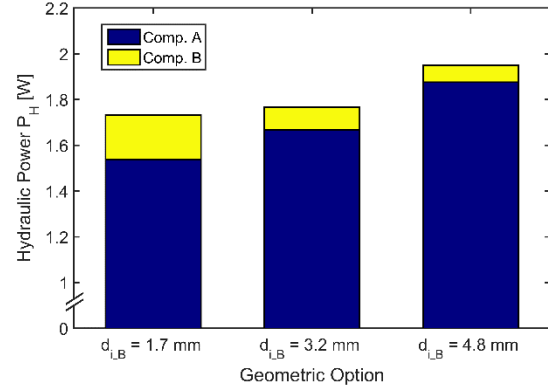


Figure 8. Power demands for the mixing of the two components in the pre-mixing chamber.

It becomes clear, that in all three cases a relatively low total power demand of about $P_H \approx 2$ W is necessary. Note that the power demand or rather the pressure loss is only slightly increasing despite the severe constriction of the component A flow cross-section in the case $d_{i_B} = 4.8$ mm (cf. Tab. 1). This is a result from the strongly non-newtonian behavior of the adhesive component A, where an increasing shear rate leads to a decreasing dynamic viscosity of the fluid. In order to verify this observation, the average shear rates of component A in the area of constriction at the inlet component B were calculated for the three geometrical options. It was found that the shear rate in this area increases by approx. 274 % at $d_{i_B} = 4.8$ mm compared to the option $d_{i_B} = 1.7$ mm.

The obtained results led to the final conclusion that the more convenient mixing behavior of the largest tested component B inlet is entirely justified by the low increase of the power demand.

5. Summary and Conclusions

The conducted simulations with COMSOL Multiphysics® led to a better understanding of the mixing behavior in the pre-mixing chamber for two-component adhesives in particular in the area of the accelerator component injection. With the simulation results a suitable design for the relevant geometrical parameter d_{i_B} could be identified. In this context the evaluation of the phase distribution revealed the result that the geometrical extent of the component B region at the outlet increases significantly with increasing diameter of the component B inlet. Concerning the power demand of the fluid technical system it was determined that the non-newtonian viscosity characteristics of the adhesive components have a significant influence where the power demand

was slightly increasing with increasing diameter of the component B inlet.

Future work will be focused on the design of the main mixing stage using adjusted static mixer elements. This will further be enabled by COMSOL Multiphysics® using the introduced mathematical model as well as the achieved results presented in this study. Finally, the validation by experimental work will be helpful for the understanding of the mechanisms in the pre-mixing chamber and for the improvement of the model quality.

References

1. R.D. Adams, J. Comyn, Joining using adhesives, *Assembly Automation*, **20**, 109-117 (2000)
2. Newborn Brothers Co., Inc., Pneumatic Dual Component, online: URL: <http://www.newborncaulkguns.com/> (2017-06)

Acknowledgements

This project is funded by the Federal Ministry of Economics and Technology, following a decision of the German Bundestag.

Nomenclature

Symbol	Parameter	Unit
$A_{A/B}$	Inlet area of comp. A/B	[m ²]
A_O	Outlet area	[m ²]
$d_{i_A/B}$	Inner diameter of comp. A/B inlet	[m]
$d_{o_A/B}$	Outer diameter of comp. A/B inlet	[m]
M	Mixing ratio comp. A:B	[-]
p	Pressure	[Pa]
$\bar{p}_{A/B}$	Average pressure at the inlet of comp. A/B	[Pa]
p_O	Pressure at the outlet	[Pa]
P_H	Hydraulic Power	[W]
\vec{v}	Fluid velocity vector	[m/s]
$v_{A/B}$	Flow velocity of comp. A/B	[m/s]
v_{A/B_inj}	Flow velocity of comp. A/B in the area of injection	[m/s]
$\dot{V}_{A/B}$	Volume flow of comp. A/B	[m ³ /s]
η	Dynamic viscosity	[Pa s]
ν	Diffusion coefficient	[m ² /s]
ρ	Fluid density	[kg/m ³]
Φ	Phase fraction	[-]